Environ Sci Pollut Res (2017) 24:15804–15815
DOI 10.1007/s11356-017-8921-9

RESEARCH ARTICLE

Leaching behavior of U, Mn, Sr, and Pb from different particle-size fractions of uranium mill tailings

Bo Liu [1,2] · **Tongjiang Peng** [2] · **Hongjuan Sun** [2]

Received: 9 September 2016 / Accepted: 23 March 2017 / Published online: 22 May 2017

Abstract Pollution by the release of heavy metals from tailings constitutes a potential threat to the environment. To characterize the processes governing the release of Mn, Sr, Pb, and U from the uranium mill tailings, a dynamic leaching test was applied for different size of uranium mill tailings samples. Inductively coupled plasma atomic emission spectroscopy (ICP-AES) and inductively coupled plasma mass spectrometry (ICP-MS) were performed to determine the content of Mn, Sr, Pb, and U in the leachates. The release of mobile Mn, Sr, Pb, and U fraction was slow, being faster in the initial stage and then attained a near steady-state condition. The experimental results demonstrate that the release of Mn, Sr, Pb, and U from uranium mill tailings with different size fractions is controlled by a variety of mechanisms. Surface wash-off is the release mechanism for Mn. The main release mechanism of Sr and Pb is the dissolution in the initial leaching stage. For U, a mixed process of wash-off and diffusion is the controlling mechanism.

Keywords Uranium mill tailings · Release behavior · Adsorption · Desorption · Mineral dissolution

Responsible editor: Georg Steinhauser

✉ Tongjiang Peng
tjpeng@swust.edu.cn

[1] School of Environment and Resource, Southwest University of Science and Technology, Mianyang 621010, Sichuan, People's Republic of China

[2] Key Laboratory of Solid Waste Treatment and Resource Recycle, Southwest University of Science and Technology, Ministry of Education, Mianyang 621010, Sichuan, People's Republic of China

Introduction

With an urgent demand for clean energy and the rapid development of the nuclear industry, many countries are engaged in uranium mining and metallurgy projects. There are more than 20 billion t of uranium mill tailings worldwide (Abreu et al. 2014; Herring 2013; Yan 2016). As a unique industrial solid waste, uranium mill tailings are radioactive and heavy metal toxic. They not only contain the residue radionuclides but also contain various kinds of heavy metals such as Mn, Cd, Cr, Ni, Sr, and Pb (Abdelouas 2006). Under certain environmental conditions, these metals will possibly be released from the tailings into the soil and water. Therefore, uranium mill tailings are potential contamination sources in surroundings, which cannot be neglected.

Elevated concentration of dissolved contaminants is an environmental concern in the uranium mining industry. For example, Northern Saskatchewan, Canada, accounts for approximately one third of the world's total uranium production (Chen et al. 2009). The mining has resulted in the production of more than 36 million t of tailings (Low-Level Radioactive Waste Management Office 2004). Their uranium tailings typically contain elevated concentrations of As, Mo, Ni, and Se which exceed health standards and potential transfer to the surrounding groundwater (Essilfie-Dughan et al. 2012; Essilfie-Dughan et al. 2010; Mahoney et al. 2007). To mitigate this problem, uranium mill effluents are neutralized with lime to reduce the aqueous concentration of these elements of concern (EOCs) (Gomez et al. 2013). After neutralization, the tailings are deposited below the groundwater table in engineered in-pit tailing management facilities that have been designed to create low hydraulic gradients across the tailings' body. This ensures that the migration of aqueous EOCs from the low hydraulic conductivity tailings to the surrounding groundwater will be dominated by diffusive transport, thus minimizing the flux of EOCs

from the tailings' body to the surrounding groundwater (Shaw et al. 2011). In China, most of the uranium mill tailings were normally dumped in the industry processed ponds on the land surface. Especially, no further treatment was taken after the uranium mill tailings were piled in the uranium mill tailings pond in the early stage (Lv et al. 2014; Wang et al. 2012a). Therefore, the uranium and associated heavy metals in the tailings will become unstable under the water environment (Liu et al. 2015). Water from surface runoff and rainfall has important impacts on various geophysical and geochemical processes. It possibly triggers a sequence of reactions and carries contaminants away from the waste sites (Al-Hashimi et al. 1996). In addition, possible water infiltration through uranium mill tailings is a potential risk to the underground aquifers (Al-Hashimi et al. 1996). Hence, it is important to estimate the leaching of heavy metals from tailings that act as the major migration and transfer processes caused by the possible infiltration of water into tailings piles.

Due to the potential environmental impacts of EOCs, research efforts have focused on the affecting factors. The mobilization and transport of EOCs from uranium mill tailings are complicated processes. Some researchers found that the release of EOCs from uranium mill tailings could be accelerated by fluoride, carbonate, and bicarbonate (Ram et al. 2013; Santos and Ladeira 2011). Other published research revealed that the stability and mobility of uranium were also impacted by pH, redox potential, and temperature (Othmane et al. 2013; Wang et al. 2012b). However, the release of uranium and associated heavy metals from these tailings primarily depends on the chemical composition of the uranium mill tailings itself. It was found that the mineralogical factors that controlled the mobility of EOCs in the uranium tailings were dominated by gypsum, two-line ferrihydrite, Mg-Al hydrotalcite, Al oxides, and poorly crystalline scorodite, among other minor secondary mineral phases that adsorb and/or precipitate EOCs (Langmuir et al. 2006; Mahoney et al. 2007; Robertson et al. 2016).

Particle size is an important property of uranium mill tailings that affects the migration and retention of solute and contaminant (Sparks 1995). Landa (1987) investigated the effect of particle size fractions on the mobility of Rn and found that coarse tailing fractions had emanation coefficients which were lower than those of their fine-fraction counterparts. Shang et al. (2011) investigated the effect of grain size on uranium surface complexation kinetics and found that uranium surface complexation kinetics were size specific. Particle size affects the length of diffusion paths (Ewing et al. 2010). It also affects the specific surface, pore volume, connectivity, and the distribution of the EOCs in intragrain domains (Flemming 2007; Sierra et al. 2011). Therefore, it may affect the release of contaminants from the sediments.

The objective of this study is to investigate leaching behavior of different particle-size fractions of uranium mill tailings at simulated acid rain condition. The study focused on Mn, Sr, Pb, and U. Mineralogical features of uranium mill tailings were characterized by X-ray diffraction (XRD). The release of U, Mn, Sr, and Pb from uranium mill tailings was simulated under semi-dynamic leaching conditions. The amount of Mn leached out from the studied matrices was determined by inductively coupled plasma atomic emission spectroscopy (ICP-AES). The amount of U, Sr, and Pb leached out from the studied matrices was determined by inductively coupled plasma mass spectrometry (ICP-MS). The processes governing the release of uranium were identified, and the bulk release of U, Mn, Sr, and Pb from the samples was also investigated. Hence, this study provides an insight into the fraction of mobile uranium and associated heavy metals leached out from waste matrices over a long time period and identifies the processes governing slow uranium leaching.

Material and methods

Sampling site

The samples were taken from a tailing impoundment affiliated to a uranium mining and metallurgy plant in the northwest China. Uranium tailings containing waste rocks, low-grade uranium ore, and residues after uranium extraction were discharged into the impoundment. They were brown-colored solids containing uranium and other heavy metal ions and were neutralized with lime. The tailing impoundment is surrounded with artificial dams (Fig. 1). It situates near a densely populated area. The study area has a subtropical humid continental climate. The average annual temperature is 9.5 °C with an extremely low temperature of −7.2 °C and extremely high temperature of 38.3 °C. The average annual rainfall in this area is about 300 mm from May to September. Tailings dump is a reactive environment that evolves with time through a large variety of physical and chemical processes. Similarly to other tailings sites in the early decades of uranium mining, no engineered cover or bottom liner was used to effectively contain the tailings. Since the tailing dumps have no protective soil cover and because of the large pore size among the tailings, the residual uranium in the tailings is directly washed out during rainfall. The elutropic uranium from the tailings dump transports to subsurface aquifers and groundwater, which is subsequently used for drinking water and irrigation purposes in the locality.

Sampling and sample preparation

Three sampling sites were selected at the uranium mill tailing pond. Samples were collected from the tailings located at the subsurface horizon with a depth of 20 cm from the surface. Collected tailings were packed into a labeled plastic boxes. In

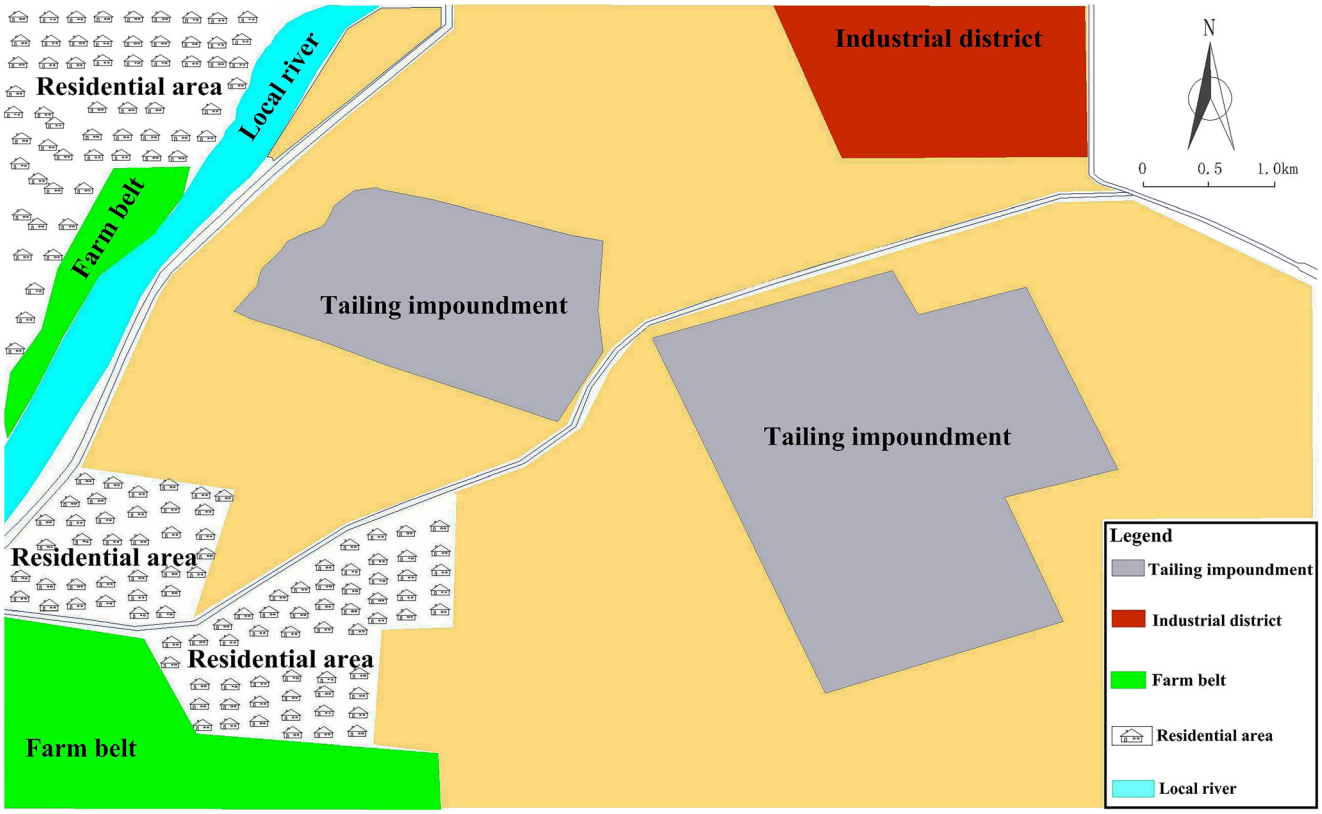

Fig. 1 Location map of uranium tailing impoundment

the laboratory, the collected tailings at three sites were blended with a mixer for 10 min and dried at room temperature for 2 weeks.

To study the release behavior of EOCs of uranium mill tailings with different natural particle sizes, uranium mill tailings were dry-sieved to four size fractions (>830, 380~830, 250~380, and <250 μm) with standard sieves. The sieved samples were marked with umt-bl-ps-20+, umt-bl-ps-20-40, umt-bl-ps-40-60, and umt-bl-ps-60−, respectively. After leached, they were nominated with umt-al-ps-20+, umt-al-ps-20-40, umt-al-ps-40-60, and umt-al-ps-60−, respectively. All chemical reagents employed in this work were analytical grade. Before the experiment, all glassware and plastics used were soaked in 10% nitric acid solution for 24 h and then cleaned repeatedly with ultra-pure water (18.25 MΩ cm; Ulupure, China). According to the ion chromatography analysis of local rainwater samples, a pH = 4.5 leaching solution using H_2SO_4 and HNO_3 with a mole ratio of 4:1 was formulated.

Column experiments

Leaching tests were performed in plexiglass tubular columns, and the schematic drawing of the columns is presented in Fig. 2. All cylindrical columns were 30 mm in internal diameter and 200 mm in total height. Coarse quartz sands (gravel layers) located on top and bottom minimize the pressure inside of the column. Fine quartz sands (stainless filters) were employed to prevent leakage of uranium mill tailings. Injection of influent and effluent ran through plexiglass tubes, and the digital pump was applied. The weight of screening samples loaded for each column was 100.00 g. The volume of tailings column was about 70.65 cm^3. Each column was flushed with 80 mL of the simulated acid rain per day at room temperature. The leaching test lasted for 50 days. Experiments were conducted in triplicate. The leachate from the column was filtered through a 0.45 μm membrane filter and stored in a 100-mL volumetric flask for later tests each day. The pH value, electrical conductivity, and metals concentration were analyzed immediately after each leachate collection.

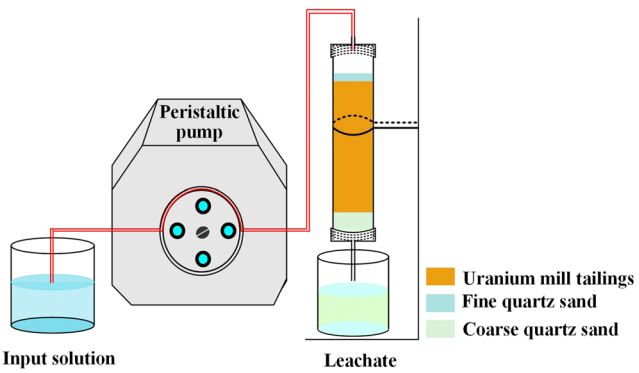

Fig. 2 The schematic drawing of the dynamic leaching test

After the final leachate measurement, the columns were separated and extruded. The soil from the entire depth range of each column was thoroughly mixed, dried, and ground for later analysis.

Characterization techniques

Crystalline mineral phases of samples were determined by using an X-ray diffractometer. The XRD measurement was conducted on a PANalytical X'Pert PRO multifunctional powder diffractometer with the Kα1 line from Cu (λ = 0.15406 nm). Each scan was done within the 2θ range from 3° to 80°, with a step size of 0.03° and a step time of 30 s. Before the XRD analysis, the samples were dried at the room temperature and ground to obtain the ≤75 μm size fraction with a pestle and mortar. A zero background and hollowed sample holder were used for powdered samples. The interpretation was done by comparing XRD patterns of the samples to those of known minerals (JCPDS XRD patterns). Compositions of the tailings were measured using Panalytical Axios wavelength dispersive X-ray fluorescence (XRF) with scintillation detector range 8°–104°. The pH and electrical conductivity were measured with a potentiometric pH meter (Rex pHS-3C) and conductivity meter (Rex DOS-307A), respectively. Quantitative chemical analyses of the EOCs in the leachate were analyzed with ICP-AES and ICP-MS. The concentration of Mn was determined by PerkinElmer Analyst 700 atomic absorption spectrometer. A de-ionized water sample was used to establish the instrument background, and four standard concentrations (5, 10, 15, 20 mg/L) were used to calibrate the unit. The ^{55}Mn was selected to develop this method. The calibration curves with $R^2 > 0.9999$ were accepted for concentration calculation. Quality control was implemented by the inclusion of reagent blanks and duplicate samples. U, Sr, and Pb concentrations were measured on an Agilent 7700X ICP-MS with a double-pass quartz spray chamber. Calibration line method was used for the quantification of U, Sr, and Pb. A de-ionized water sample was used to establish the instrument background, and eight standard concentrations (10, 20, 50, 100, 200, 500, 1000 μg/L) were used to calibrate the unit. The isotopes ^{238}U, ^{88}Sr, and ^{208}Pb were selected to develop this method. The calibration curves with $R^2 > 0.9999$ were accepted for concentration calculation. Quality control was implemented by the inclusion of reagent blanks and duplicate samples.

Statistical analysis

The correlation analysis was performed with the SPSS 22 software package. The correlation coefficient is statistically significant at 95 and 99% significance level. The two-sided hypothesis was used in this study.

Results and discussion

Mineralogy of the uranium mill tailings

The mineralogical information of uranium mill tailings was critical to understanding uranium genesis and to developing appropriate management methods in the stabilization of uranium and toxic metals. Therefore, attempts have been undertaken to study the mineralogical characteristics of uranium mill tailings. Due to the grain-size distribution, uranium mill tailings were mainly sieved into four size fractions: gravel sand (>0.83 mm), coarse sand (0.38–0.83 mm), medium sand (0.25–0.38 mm), and fine sand (<0.25 mm). The tailings consisted of 50.9 ± 5% gravel sand. The other size fractions consisted of 31.1 ± 8, 9.5 ± 1, and 8.5 ± 4% of coarse sand, medium sand, and fine sand, respectively. The major minerals detected by the XRD were the same for all size fractions: quartz, gypsum, albite, and minor amounts of clinochlore. Major mineral components in our samples are similar to the XRD analysis of Othmane's sample (Othmane et al. 2013). The albite, quartz, and clinochlore in the samples are the original silicate and clay gangue minerals. The occurrence of gypsum is probably a secondary mineral which is related to the dissolution of calcite in the ore with sulfuric acid during the uranium leaching process and the precipitation from neutralization (Fig. 3). No uranium-bearing mineral phase is positively identified in all samples with XRD. It revealed that the uranium may exist in the form of isomorphic substitution or adsorption on the surface of other materials. The most significant difference in the mineralogical composition of the samples is the different contents of gypsum. Gypsum concentration was the lowest in the biggest size fraction of tailings, and it increased with decreasing size fractions. This indicated that the distribution of minerals in different size fraction samples is size specific. After the entrained acidic water co-disposed with

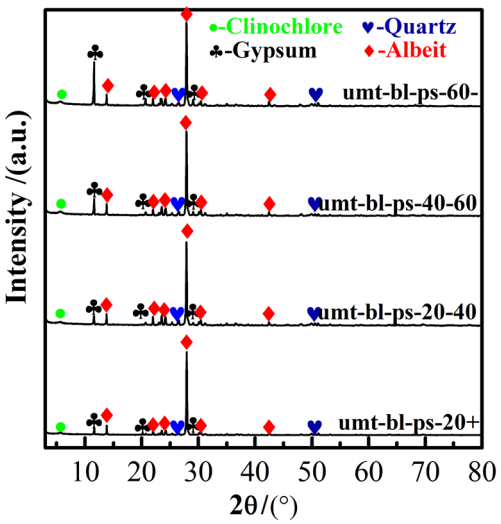

Fig. 3 XRD of the pre-leaching samples with different natural sizes

uranium tailings, most of the X-ray diffraction of gypsum is under the detection limit of XRD (Fig. 4), suggesting that the gypsum minerals are dissolved. The same result is confirmed by another study (Silver 1985). The dissolution of gypsum occurs because the incoming water is under saturated with it (Zhu et al. 2001). Additionally, the clinochlore in samples also reduced because acids cause clay dissolution (Szecsody et al. 2013).

Chemical compositions of the tailings were investigated with X-ray fluorescence analysis (Table 1). The principal chemical components in tailings were SiO_2, Al_2O_3, Na_2O, CaO, Fe_2O_3, and S. These chemical components were corresponding to the quartz, albite, gypsum, and clinochlore minerals. The contents of CaO and S increased with the decrease of the particle size. This was a line with the XRD analysis. Minor quantities of metallic elements such as Ba, Mn, Sr, Pb, and U were identified. Considering the environmental effect of metallic elements (Mcarthur et al. 2012; Singh et al. 2011), Mn, Sr, Pb, and U were chosen to be the EOCs.

Fractionation of U, Mn, Sr, and Pb

To obtain the exact content of uranium in our uranium mill tailings samples, samples were digested with HNO_3 and HF. The U, Mn, Sr, and Pb in the digestion solution were detected with ICP-MS. The contents of U, Mn, Sr, and Pb in the particle-size samples are displayed in Fig. 5. Each toxic metal differs among different size fractions, indicating that particle size affects the distribution of the selected metals.

The distribution of heavy metals primarily depends on the mineral composition and adsorption sites in different size fractions. With regard to the contribution of different size samples, the small size sample (umt-bl-ps-60−) was found to be the major fraction responsible for metal accumulation, due to the high specific surface area (Sutherland 2003). In addition, the

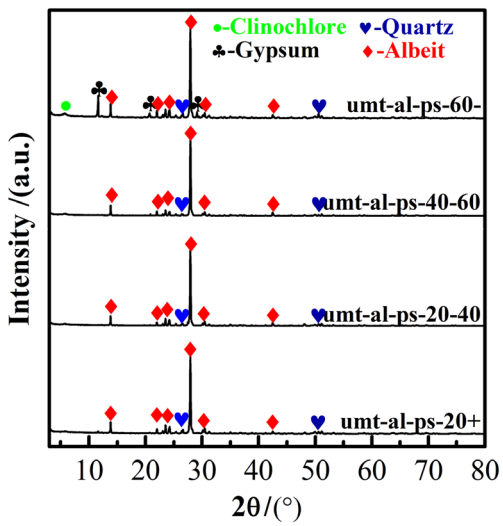

Fig. 4 XRD of the leached samples with different natural sizes

mean concentration of U, Sr, Pb, and Mn in all samples descended in the order of Mn > Sr > U > Pb.

The bioavailability, mobility, and toxicity of U, Mn, Sr, and Pb were affected by their distributions as well as their total concentrations (Lee and Touray 1998). Therefore, it is necessary to analyze the fractionation of U, Mn, Sr, and Pb for identification of the potential release behavior (Fig. 6).

The water-soluble and exchangeable fractions contain water-soluble species such as the free ion and weakly adsorbed species. They represent the most mobile and potentially most available species in the environment (Rout et al. 2016; Vandenhove et al. 2014). Therefore, metals associated with water-soluble and exchangeable fractions in the sample could be released, and find it easy to migrate within the environment under neutral conditions (Singh et al. 2015).

The fraction of Mn (Fig. 6a) for all the particle-size samples indicates that most Mn is associated with the residue, water-soluble, and exchangeable fraction. The average value of the labile fraction (water-soluble and exchangeable fractions) for Mn follows the order in the particle-size samples: 52.7 ± 2% (umt-bl-ps-60−) > 49.5 ± 1% (umt-bl-ps-20-40) > 48.5 ± 2% (umt-bl-ps-40-60) > 41.0 ± 3% (umt-bl-ps-20+). Most Pb is associated with the residue fraction (Fig. 5b), and the share of mobile fractions is low (Fig. 6b). For different samples, the labile fraction of Pb is decreased with the order of 16.9 ± 1% (umt-bl-ps-40-60) > 9.4 ± 1% (umt-bl-ps-20-40) > 3.7 ± 2% (umt-bl-ps-20+) > 3.1 ± 1% (umt-bl-ps-60−). Most Sr is associated with the residue, water-soluble, and exchangeable fraction (Fig. 6c). It seems that the high concentration of Sr has been found associated with the labile fractions in all samples. The decreasing order is 59.3 ± 4% (umt-bl-ps-40-60) > 55.2 ± 1% (umt-bl-ps-20-40) > 46.6 ± 2% (umt-bl-ps-20+) > 43.9 ± 2% (umt-bl-ps-60−). The fraction of U (Fig. 6d) indicates that the high concentration of U has been found associated with the residue fraction in all samples. A small amount of U is in the labile fractions with the decreasing order of 6.4 ± 1% (umt-bl-ps-40-60) > 5.4 ± 2% (umt-bl-ps-20-40) > 4.9 ± 1% (umt-bl-ps-20+) > 3.0 ± 2% (umt-bl-ps-60−). From the distributions of U, Mn, Sr, and Pb, it may be assumed that under environmental conditions Mn and Sr are more readily released than Pb and U.

pH and conductivity of effluents

During the leaching process, the effluents were within pH 4.2 to 6.8 (Fig. 7). With elution time went on, the pH of effluents was higher than that of influents (pH = 4.5), indicating that acid was continuously consumed. However, acid consumptions of four columns were different. The pH of leachate from the fine-grained fractions exceeded other size samples. It implied that the acid neutralization ability of fine-grained uranium mill tailing sample was stronger than that of the coarse size ones. This could be attributed to the highest content of

Table 1 Chemical components of the uranium mill tailings

No.	umt-bl-ps-20+	umt-bl-ps-20-40	umt-bl-ps-40-60	umt-bl-ps-60−
SiO_2	65.9 ± 0.3%	62 ± 0.3%	61.4 ± 0.5%	58.9 ± 0.9%
Al_2O_3	18.7 ± 0.5%	17.9 ± 0.5%	17.5 ± 0.2%	16.9 ± 0.1%
Fe_2O_3	2.5 ± 0.6%	2.2 ± 0.4%	2.3 ± 0.2%	2.7 ± 0.4%
MgO	0.3 ± 0.1%	0.4 ± 0.1%	0.4 ± 0.1%	0.3 ± 0.1%
CaO	0.4 ± 0.2%	2.8 ± 0.5%	3.1 ± 0.5%	4.5 ± 0.5%
Na_2O	12.0 ± 0.8%	10.9 ± 0.9%	9.6 ± 0.7%	8.7 ± 0.5%
K_2O	0.3 ± 0.1%	0.2 ± 0.1%	0.2 ± 0.1%	0.2 ± 0.1%
P	618.4 ± 11.8 ppm	577.9 ± 9.6 ppm	646.0 ± 9.4 ppm	771.5 ± 5.8 ppm
S	758.8 ± 21.8 ppm	12,053.3 ± 19.8 ppm	14,886.5 ± 21.8 ppm	19,726.1 ± 15.7 ppm
Ba	235.1 ± 8.9 ppm	152.2 ± 8.7 ppm	299.5 ± 2.4 ppm	268.8 ± 9.2 ppm
Mn	141.8 ± 3.4 ppm	152.5 ± 8.9 ppm	165.7 ± 6.8 ppm	170.6 ± 4.8 ppm
Sr	100.8 ± 6.3 ppm	150.6 ± 2.8 ppm	154.4 ± 8.7 ppm	160.9 ± 5.6 ppm
Pb	60.8 ± 2.4 ppm	72.8 ± 5.8 ppm	77.2 ± 8.4 ppm	76.4 ± 6.4 ppm
U	98.6 ± 5.7 ppm	101.8 ± 4.9 ppm	106.8 ± 4.8 ppm	108.5 ± 6.1 ppm
LOI	1.0 ± 0.2%	3.1 ± 0.5%	4.2 ± 0.3%	5.7 ± 0.4%

gypsum in fine-grained samples and the dissolution of gypsum mineral in acid solutions (Calmanovici et al. 1993; Zhang and Muhammed 1989).

The conductivity of the leachate is associated with the concentration of ions. The conductivity increased with the increase of the ionic concentration (Fig. 8). The electrical conductivity of the leachate was higher than that of the influent, which indicated that the ion transport or chemical reaction occurred in the uranium mill tailings. During the penetration process in the column tailings, the influent brought out a large number of ions and salts, which led to the changes of the leachate conductivity. Conductivities of leachates from the different particle size samples were essentially consistent, keeping a trend from high to low as the time went on.

In the initial leaching stage, the conductivity of leachate was the maximum. It could be attributed to the dissolved ions in pore water. In the course of time by leaching process, the conductivity declined. It was related to the soluble minerals or soluble ions located in the uranium mill tailings. When the leaching liquid permeated, the soluble ions were quickly dissolved, making a higher electrical conductivity. However, the changes of conductivity in leachates became smaller basically after five leaching days (except umt-al-ps-60−), indicating that the rapid release stage (metals from easily dissolved metal salts) was finished and the slow release of metals from tailings went on to attain a near balance state. Although the release attains a basic balance, the conductivity still had slight changes. This result indicated that the release and migration of ions in uranium tailings were a long and slow process.

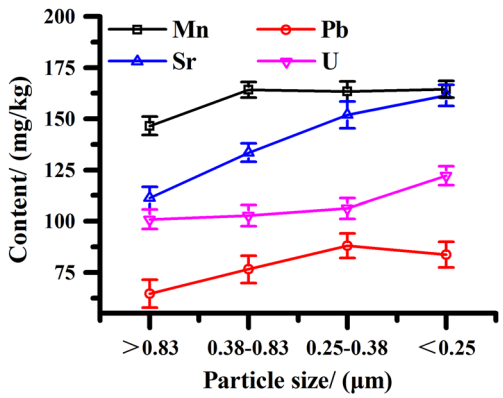

Fig. 5 Concentrations of U, Mn, Sr, and Pb in the particle-size samples

Release characteristics of U, Mn, Sr, and Pb

The release of leachate EOCs concentration versus elution time is shown in Fig. 9. The concentration changes of EOCs were consistent with the changes of conductivity in the leachate (Fig. 8). Leachate concentrations of Mn, Sr, Pb, and U decreased with increasing elution time on the whole. The maximum concentrations of Mn, Pb, and U in the leachate were far beyond drinking water quality guidance limits ruled by World Health Organization (WHO) (0.1, 0.01, and 0.002 mg/L, respectively). These results indicated that uranium mill tailings could result in the pollution of surroundings by Mn, Pb, and U through leaching. The maximum concentrations of Mn, Sr, Pb, and U in the leachate were in the order of Mn > Sr > U > Pb. This was mainly attributed to the higher concentrations of Mn and Sr in the samples. The steeper gradients of Mn and U compared to those of Sr and Pb for each treatment indicated that Mn and U were leached from tailings at a faster rate than Sr and Pb before ten leaching days. This could be

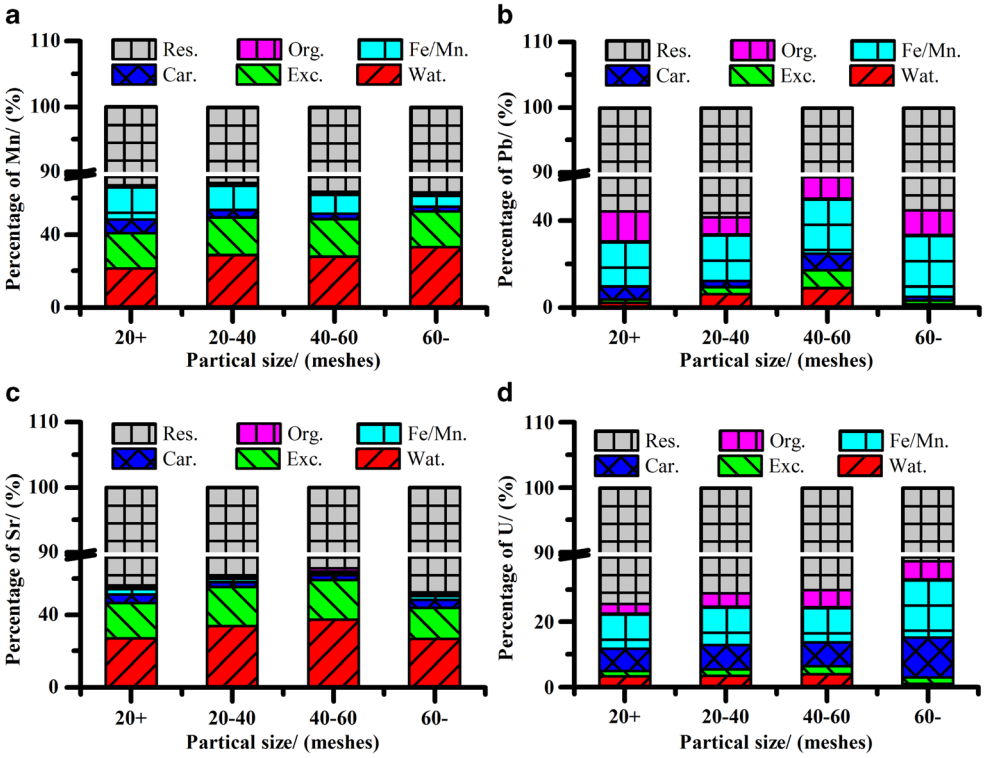

Fig. 6 Species distribution of Mn, Pb, Sr, and U in the particle-size samples. **a** Fractions of Mn. **b** Fractions of Pb. **c** Fractions of Sr. **d** Fractions of U

related with the fractionation of U, Mn, Sr, and Pb in the tested tailings. As can be seen from Fig. 9, the results indicate an initial fast leaching followed by slow leaching. This behavior suggests the presence of two different release mechanisms for the fast and slow components.

Numerous factors, such as environmental conditions, mineralogical properties of tailings, and the occurrence of elements affected the release of EOCs from uranium tailings (Landa 2004; Wang and Mulligan 2006). The particle size was one of the crucial factors affecting the leaching rate. Generally, the smaller the size of mineral particles, the higher the leaching rate of the mineral (Hariprasad et al. 2007). According to the cumulative release amount of ions (Fig. 10), the changing trends for the release of Mn, Sr, Pb, and U were in two ways. The release of Mn increased with the decrease of the tailings' particle size. However, the cumulative leaching amount of Sr, Pb, and U did not meet this regular. The cumulative leaching amount of Mn in particle-size samples follows the order: umt-al-pz-60− > umt-al-pz-40-60 ≈ umt-al-pz-20-40 > umt-al-pz-20+. For the cumulative leaching amounts of Sr, Pb, and U, the order is umt-al-pz-40-60− > umt-al-pz-20-40 > umt-al-pz-20+ > umt-al-pz-60−. This is consistent with the analysis of labile fractions. Therefore, the release behavior of Mn, Sr, Pb, and U is attrib-

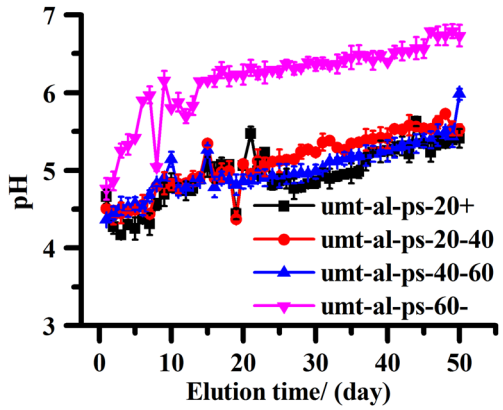

Fig. 7 pH of effluent samples

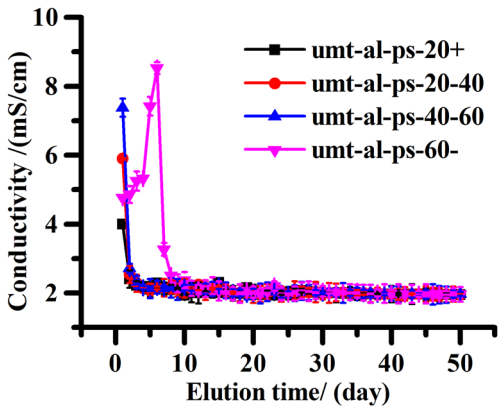

Fig. 8 Conductivity of effluent samples

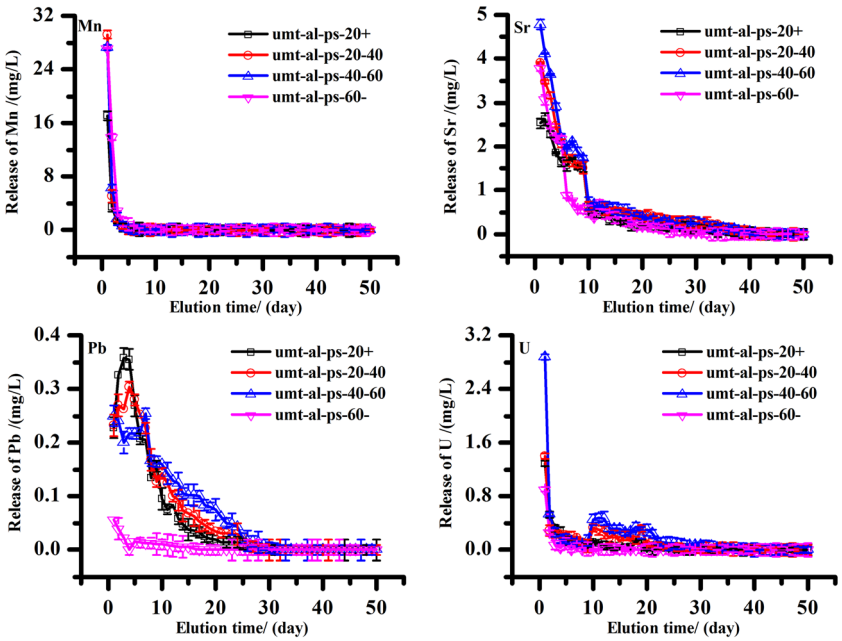

Fig. 9 The release concentration of Mn, Sr, Pb, and U

uted to the heterogeneous distribution of Mn, Sr, Pb, and U in the particle-size samples.

Leaching mechanism of Mn, Sr, Pb, and U

The release and migration of Mn, Sr, Pb, and U from uranium mill tailings are due to a variety of mechanisms. According to Fick's diffusion theory (Rahman et al. 2007), the migration of elements under semi-dynamic conditions could be explained with surface wash-off, dissolution, and diffusion. In order to determine the controlling leaching mechanisms of EOC release, a model developed by Wang was used (Wang et al. 2012b). The controlling leaching mechanism was determined based on the slope of the linear regression of the logarithm of cumulative release versus the logarithm of elution time. If the slope is less than 0.35, the controlling leaching mechanism

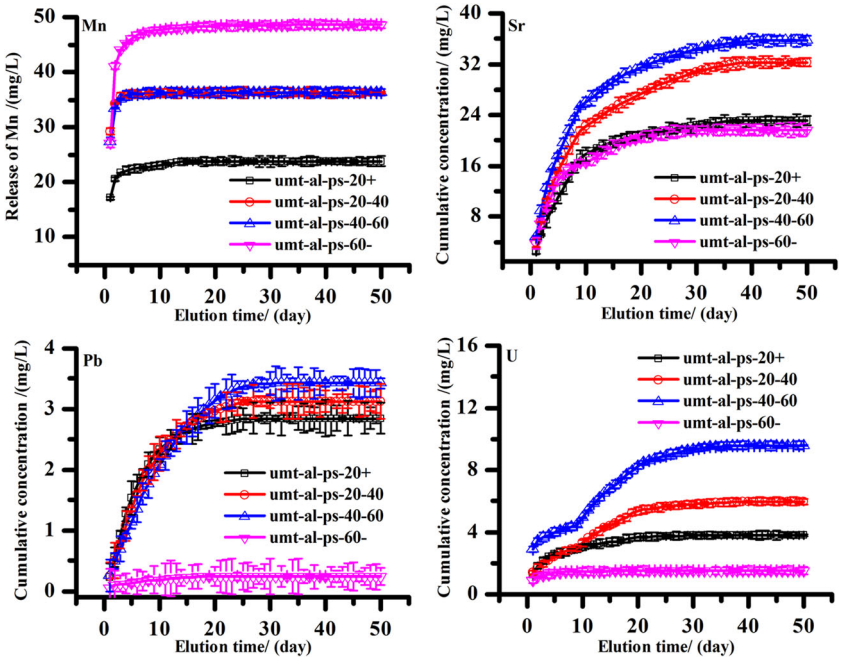

Fig. 10 Cumulative release of Mn, Sr, Pb, and U

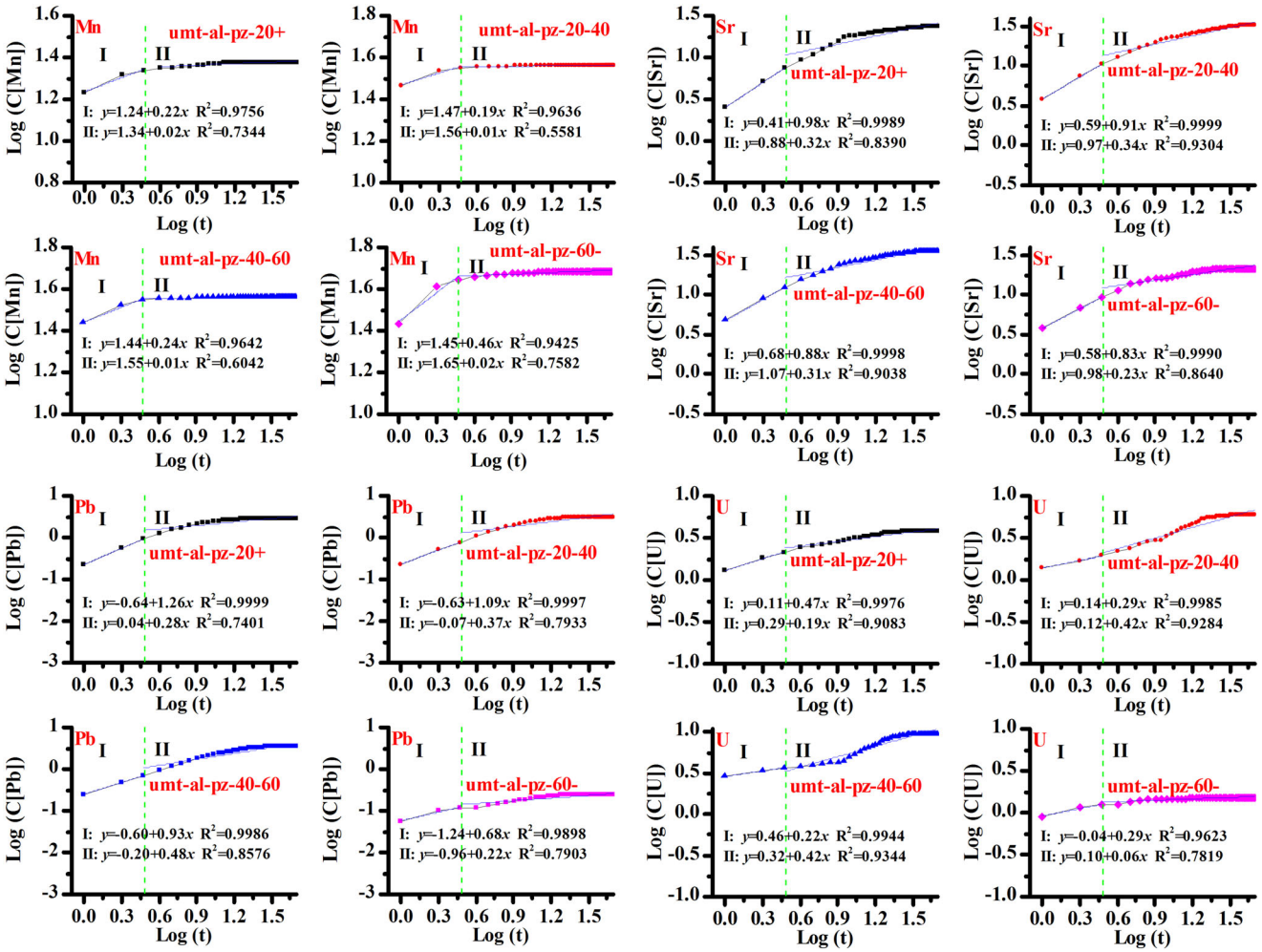

Fig. 11 Plot of log cumulative release versus elution time

will be the surface wash-off. If the slope value is located between 0.35 and 0.65, the controlling mechanism will be the diffusion. The slope value higher than 0.65 represents dissolution mechanism (Patra et al. 2011; Rahman et al. 2007).

Table 2 Release mechanism of considered elements for different particle sizes

	I-stage		II-stage		I-stage		II-stage	
	Slope	Mechanism	Slope	Mechanism	Slope	Mechanism	Slope	Mechanism
Metals	umt-al-pz-20+				umt-al-pz-20-40			
Mn	0.22	Wash-off	0.02	Wash-off	0.19	Wash-off	0.01	Wash-off
Sr	0.98	Dissolution	0.32	Wash-off	0.91	Dissolution	0.34	Wash-off
Pb	1.26	Dissolution	0.28	Wash-off	1.09	Dissolution	0.37	Diffusion
U	0.47	Diffusion	0.19	Wash-off	0.29	Wash-off	0.42	Diffusion
Metals	umt-al-pz-40-60				umt-al-pz-60–			
Mn	0.24	Wash-off	0.01	Wash-off	0.46	Diffusion	0.02	Wash-off
Sr	0.88	Dissolution	0.31	Wash-off	0.83	Dissolution	0.23	Wash-off
Pb	0.93	Dissolution	0.48	Diffusion	0.68	Dissolution	0.22	Wash-off
U	0.22	Wash-off	0.42	Diffusion	0.29	Wash-off	0.06	Wash-off

Table 3 Pearson's correlation of Mn, Sr, Pb, and U in umt-al-pz-20+ sample

>20 meshes	Mn	Sr	Pb	U
Mn	1			
Sr	0.535**	1		
Pb	0.373**	0.957**	1	
U	0.946**	0.733**	0.622**	1

*Significant at 95% level; **significant at 99% level

Table 5 Pearson's correlation of Mn, Sr, Pb, and U in umt-al-pz-40-60 sample

40–60 meshes	Mn	Sr	Pb	U
Mn	1			
Sr	0.649**	1		
Pb	0.399**	0.871**	1	
U	0.944**	0.635**	0.520**	1

*Significant at 95% level; **significant at 99% level

A log plot of the cumulative release versus elution time exhibits a power-law relationship for all size fractions (Fig. 11). Due to a series of kinetic reactions, the release of ions from the uranium mill tailings was regulated by a variety of mechanisms. With leachate diffusion in uranium mill tailings, the dissolved oxygen, water, and proton would react with uranium mill tailings by a variety of physical and chemical reactions, leading to the dissolution of free ions, the diffusion of partial exchange ions, and the secondary adsorption on the surface of the solid phase.

An initial resistance to diffusion was recognizable in the case of some metals due to an initial surface-washing period (Crank 1957). Due to the slope ranged from 0.19 to 0.46 (Table 2), Mn release was controlled by a mixed process of wash-off and diffusion for different particle-size fraction samples in stage I (leaching time at start 1–3 days). Wash-off appeared to be the main controlling mechanism for Mn because most of the slope values were below 0.35. The Sr had slope values that ranged from 0.83 to 0.98 for all particle size fractions samples. These slopes indicate that Sr leachability was dissolution controlled in the stage I. Similarly, Pb release from all particle size fractions samples was also dissolution controlled in the initial stage since all slope values were beyond 0.65. Dissolution processes of Sr and Pb were resulted both from the pore water and from the surface of the uranium tailings (Moon et al. 2009). Therefore, the release rate of Pb and Sr was slower than that of Mn. The slope of U changed from 0.22 to 0.47 in the initial stage. This indicated that U release was controlled by a mixed process of wash-off and diffusion in the initial phase of leaching. The processes governing the release of uranium from uranium tailings coincided with the results of Patra et al. (2011).

Slope values were lower than 0.35 for Mn and Sr in all size fractions during the stage I leaching process from Table 2. This indicated that the wash-off was the controlling leaching mechanism for them. The slope for Pb was close to 0.35, indicating that the leaching of lead was mainly governed by diffusion phenomenon in the post-stage. Similar results are reported by other studies (Moon and Dermatas 2006; Moon et al. 2009).

Correlation analysis of Mn, Sr, Pb, and U

In the leaching process, elements like Mn, Sr, Pb, and U were released with one or more forms into the water and would influence each other. Through the correlation analysis of Mn, Sr, Pb, and U with leaching concentration, the geochemical behavior and interaction of Mn, Sr, Pb, and U in different particle sizes of uranium tailings were revealed. Statistical analyses were performed using SPSS. Pearson's correlation coefficients were evaluated to investigate the element correlations as provided in Tables 3, 4, 5, and 6.

In general, Mn, Sr, Pb, and U were positively correlated with each other in all of the fraction samples, which may suggest a common origin. In the umt-al-pz-20+ sample group, a significantly positive correlation at 99% level was found between the elemental pairs Sr-Pb (0.957) and Mn-U

Table 4 Pearson's correlation of Mn, Sr, Pb, and U in umt-al-pz-20-40 sample

20–40 meshes	Mn	Sr	Pb	U
Mn	1			
Sr	0.599**	1		
Pb	0.340*	0.912**	1	
U	0.888**	0.713**	0.587**	1

*Significant at 95% level; **significant at 99% level

Table 6 Pearson's correlation of Mn, Sr, Pb, and U in umt-al-pz-60– sample

<60 meshes	Mn	Sr	Pb	U
Mn	1			
Sr	0.790**	1		
Pb	0.896**	0.897**	1	
U	0.975**	0.761**	0.865**	1

*Significant at 95% level; **significant at 99% level

(0.946). In the other particle-size fraction samples, Sr was also significantly positively correlated with Pb, and Mn significantly positively correlated with U. These indicated that Sr with Pb and Mn with U may have similar release behavior. The analysis of Pearson's correlation coincided with the results of release characteristics of U, Mn, Sr, and Pb.

Conclusions

The release of Mn, Sr, Pb, and U from particle-size uranium mill tailings was evaluated with leaching tests. The mineral compositions for all pre-leaching fractions were the same. However, the content of each mineral in different particle size samples was heterogeneous. The release of mobile uranium and concerned heavy metal fractions from the samples was faster in the initial stage and then attained a near steady-state condition. The processes governing the release of Mn under the experimental conditions have been identified to be surface wash-off. The release mechanism of Sr and Pb is the dissolution and wash-off. U release was controlled by a mixed process of wash-off and diffusion.

Acknowledgements The study is funded by the National Natural Science Foundation of China (Grant No. 41372052).

References

Abdelouas A (2006) Uranium mill tailings: geochemistry, mineralogy, and environmental impact. Elements 2(6):335–341

Abreu MM, Lopes J, Santos ES, Magalhães MCF (2014) Ecotoxicity evaluation of an amended soil contaminated with uranium and radium using sensitive plants. J Geochem Explor 142:112–121

Al-Hashimi A, Evans GJ, Cox B (1996) Aspects of the permanent storage of uranium tailings. Water Air Soil Pollut 88(1):83–92

Calmanovici CE, Gabas N, Laguerie C (1993) Solubility measurements for calcium sulfate dihydrate in acid solutions at 20, 50, and 70 °C. J Chem Eng Data 38(4):534–536

Chen N, Jiang DT, Cutler J, Kotzer T, Jia YF, Demopoulos GP, Rowson JW (2009) Structural characterization of poorly-crystalline scorodite, iron(III)-arsenate co-precipitates and uranium mill neutralized raffinate solids using X-ray absorption fine structure spectroscopy. Geochim Cosmochim Ac 73(11):3260–3276

Crank J (1957) The mathematics of diffusion. Oxford University Press, London and New York

Essilfie-Dughan J, Pickering IJ, Hendry MJ, George GN, Kotzer T (2010) Molybdenum speciation in uranium mine tailings using X-ray absorption spectroscopy. Environ Sci Technol 45(2):455–460

Essilfie-Dughan J, Hendry MJ, Warner J, Kotzer T (2012) Microscale mineralogical characterization of As, Fe, and Ni in uranium mine tailings. Geochim Cosmochim Ac 96(11):336–352

Ewing RP, Hu Q, Liu C (2010) Scale dependence of intragranular porosity, tortuosity, and diffusivity. Water Resour Res 46(6):w06513

Flemming BW (2007) The influence of grain-size analysis methods and sediment mixing on curve shapes and textural parameters: implications for sediment trend analysis. Sediment Geol 202(3):425–435

Gomez MA, Hendry MJ, Koshinsky J, Essilfie-Dughan J, Paikaray S, Chen J (2013) Mineralogical controls on aluminum and magnesium in uranium mill tailings: Key Lake, Saskatchewan, Canada. Environ Sci Technol 47(14):7883–7891

Hariprasad D, Dash B, Ghosh MK, Anand S (2007) Leaching of manganese ores using sawdust as a reductant. Miner Eng 20(14):1293–1295

Herring JS (2013) Uranium and thorium resources. In: Tsoulfanidis N (ed) Nuclear energy. Springer, New York, pp 463–490

Landa ER (1987) Radium-226 contents and Rn emanation coefficients of particle-size fractions of alkaline, acid and mixed U mill tailings. Health Phys 52:303–310

Landa ER (2004) Uranium mill tailings: nuclear waste and natural laboratory for geochemical and radioecological investigations. J Environ Radioactiv 77(1):1–27

Langmuir D, Mahoney J, Rowson J (2006) Solubility products of amorphous ferric arsenate and crystalline scorodite ($FeAsO_4{\cdot}2H_2O$) and their application to arsenic behavior in buried mine tailings. Geochim Cosmochim Ac 70(12):2942–2956

Lee PK, Touray JC (1998) Characteristics of a polluted artificial soil located along a motorway and effects of acidification on the leaching behavior of heavy metals (Pb, Zn, Cd). Water Res 32(11):3425–3435

Liu J, Wang J, Li H, Shen CC, Chen Y, Wang C, Ye H, Long J, Song G, Wu Y (2015) Surface sediment contamination by uranium mining/milling activities in South China. CLEAN-Soil Air Water 43(3):414–420

Low-Level Radioactive Waste Management Office (2004) Inventory of radioactive waste in Canada. Ottawa, Canada

Lv JW, Deng QW, Zhang Y (2014) Influence of radionuclides on farmland soil and creek sediment around a uranium mine in the southwest of China. Appl Mech Mater 455:23–27

Mahoney J, Slaughter M, Langmuir D, Rowson J (2007) Control of As and Ni releases from a uranium mill tailings neutralization circuit: solution chemistry, mineralogy and geochemical modeling of laboratory study results. Appl Geochem 22:2758–2776

Mcarthur JM, Sikdar PK, Nath B, Grassineau N, Marshall JD, Banerjee DM (2012) Sedimentological control on Mn, and other trace elements, in groundwater of the bengal delta. Environ Sci Technol 46(2):669–676

Moon DH, Dermatas D (2006) An evaluation of lead leachability from stabilized/solidified soils under modified semi-dynamic leaching conditions. Eng Geol 85(1):67–74

Moon DH, Dermatas D, Grubb DG (2009) Release of arsenic (As) and lead (Pb) from quicklime-sulfate stabilized/solidified soils under diffusion-controlled conditions. Environ Monit Assess 169(1):259–265

Othmane G, Allard T, Morin G, Sélo M, Brest J, Llorens I, Chen N, Bargar JR, Fayek M, Calas G (2013) Uranium association with iron-bearing phases in mill tailings from Gunnar. Canada Environ Sci Technol 47(22):12695–12702

Patra AC, Sumesh CG, Mohapatra S, Sahoo SK, Tripathi RM, Puranik VD (2011) Long-term leaching of uranium from different waste matrices. J Environ Manag 92(3):919–925

Rahman RA, Zaki AA, El-Kamash AM (2007) Modeling the long-term leaching behavior of ^{137}Cs, ^{60}Co, and $^{152,154}Eu$ radionuclides from cement-clay matrices. J Hazard Mater 145(3):372–380

Ram R, Charalambous F, McMaster S, Tardio J, Bhargava SK (2013) An investigation on the effects of several anions on the dissolution of synthetic uraninite (UO_2). Hydrometallurgy 136:93–104

Robertson J, Hendry MJ, Essilfie-Dughan J, Chen J (2016) Precipitation of aluminum and magnesium secondary minerals from uranium mill raffinate (pH 1.0-10.5) and their controls on aqueous contaminants. Appl Geochem 64:30–42

Rout S, Kumar A, Ravi PM, Tripathi RM (2016) Understanding the solid phase chemical fractionation of uranium in soil and effect of ageing. J Hazard Mater 317:457–465

Santos EA, Ladeira AC (2011) Recovery of uranium from mine waste by leaching with carbonate-based reagents. Environ Sci Technol 45(8): 3591–3597

Shang J, Liu C, Wang Z, Zachara JM (2011) Effect of grain size on uranium (VI) surface complexation kinetics and adsorption additivity. Environ Sci Technol 45(14):6025–6031

Shaw SA, Hendry MJ, Essilfie-Dughan J, Kotzer T, Wallschläger D (2011) Distribution, characterization, and geochemical controls of elements of concern in uranium mine tailings, Key lake, Saskatchewan, Canada. Appl Geochem 26(12):2044–2056

Sierra C, Menéndez-Aguado JM, Afif E, Carrero M, Gallego JR (2011) Feasibility study on the use of soil washing to remediate the As-Hg contamination at an ancient mining and metallurgy area. J Hazard Mater 196:93–100

Silver M (1985) Water leaching characteristics of uranium tailings from Ontario and Northern Saskatchewan. Hydrometallurgy 14(2):189–217

Singh R, Gautam N, Mishra A, Gupta R (2011) Heavy metals and living systems: an overview. Indian J Pharmacol 43(3):246

Singh KL, Sudhakar G, Swaminathan SK, Rao CM (2015) Identification of elite native plants species for phytoaccumulation and remediation of major contaminants in uranium tailing ponds and its affected area. Environ Dev Sust 17(1):57–81

Sparks DL (1995) Environmental soil chemistry. Academic Press, Inc., San Diego

Sutherland RA (2003) Lead in grain size fractions of road-deposited sediment. Environ Pollut 121(2):229–237

Szecsody JE, Truex MJ, Qafoku NP, Wellman DM, Resch T, Zhong L (2013) Influence of acidic and alkaline waste solution properties on uranium migration in subsurface sediments. J Contam Hydrol 151: 155–175

Vandenhove H, Vanhoudt N, Duquène L, Antunes K, Wannijn J (2014) Comparison of two sequential extraction procedures for uranium fractionation in contaminated soils. J Environ Radioactiv 137:1–9

Wang S, Mulligan CN (2006) Occurrence of arsenic contamination in Canada: sources, behavior and distribution. Sci Total Environ 366(2):701–721

Wang J et al (2012a) Surface water contamination by uranium mining/milling activities in northern Guangdong province, China. CLEAN-Soil, Air, Water 40(12):1357–1363

Wang J et al (2012b) Uranium and thorium leached from uranium mill tailing of Guangdong province, China and its implication for radiological risk. Radiat Prot Dosim 152(1–3):215–219

Yan X (2016) Uptake of radionuclide thorium by twelve native plants grown in uranium mill tailings soils from south part of China. Nucl Eng Des 304:80–83

Zhang Y, Muhammed M (1989) Solubility of calcium sulfate dihydrate in nitric acid solutions containing calcium nitrate and phosphoric acid. J Chem Eng Data 34(1):121–124

Zhu C, Hu FQ, Burden DS (2001) Multi-component reactive transport modeling of natural attenuation of an acid groundwater plume at a uranium mill tailings site. J Contam Hydrol 52(1):85–108